MODELING THE HEAT DISTRIBUTION OF A COMPOSITE LAMINATE DURING ULTRASONIC COMPACTION WITH THE PGD

J. Justo[a*], F. Chinesta[b], E. Graciani[a], Ch. Ghnatios[b], F. París[a]

[a]*Grupo de Elasticidad y Resistencia de Materiales, Escuela Técnica Superior de Ingenieros, Universidad de Sevilla, Camino de los descubrimientos, s/n, 41092, Sevilla, España.*
[b]*Institut de recherche en génie civil et mécanique, École Centrale de Nantes, Francia.*
**jjusto@us.es*

Keywords: Composites, Ultrasonic compaction, PGD.

Abstract

New out-of-autoclave layer-by-layer curing techniques require the use of an in-situ compaction device. Ultrasonic compaction can be a suitable system to achieve this goal.
In the ultrasonic compaction, a pressure cylinder is excited over the composite laminate at a certain frequency. The vibration produces the heating of the resin of the plies, due to the internal viscosity of the polymer. The knowledge of how this heat is generated and distributed throughout the laminate is an important factor in the understanding of the ultrasonic compaction procedure.
In this work, the development and implementation of a proper generalized decomposition (PGD) model to solve the heat generation and distribution during the ultrasonic compaction is presented.
The results of the model will be presented and will be compared with experimental measurements, showing that the model can predict the temperature field properly.

1. Introduction

The ultrasonic compaction is a new system whose aim is to compact composite laminates and it should be an alternative to the common vacuum bags used in the autoclave manufacturing [1]. It offers the possibility to compact the laminates in the same process than the plies are placed, so it could be also a good technology to be coupled with the new out-of-autoclave curing techniques, like plasma beams or low energy electron beams [2], in which the curing process is made layer-by-layer.

In the ultrasonic compaction, a sonotrode with a titanium tip is excited over the composite laminate, making the resin to vibrate at an ultrasonic frequency. This excitation makes the resin to rise its temperature, due to its internal viscosity. The heating facilitates the air bubbles trapped between the plies to scape, achieving the compaction of the part. The modeling of how the heat is generated and distributed inside the laminate will help to model and optimize the ultrasonic compaction process.

The heat generation was studied in previous works [3, 4, 5], leading to a model that estimates this heat as a function of the viscosities and vertical velocities of the resin layers of the laminate. This model will be used in this work.

In the case of the heat distribution, the problem will be solved with the Proper Generalized Decomposition (PGD) [6, 7], using the equations that will be presented in section 4 of this paper. The need of fine meshes in terms of space (to model the thickness of the resin and fibre layers) and time (to model properly the ultrasonic oscillation along the whole compaction process) makes the PGD a suitable option for solving the heat equation.

The problem to be studied is presented in section 2 where the geometry and the boundary conditions of the laminate under study will be shown.

The way of coupling the heat generation and the heat distribution problems and the equations that solve the heat distribution with the PGD will be stated in sections 3 and 4, respectively. The results of the coupled heat generation and distribution problem will be shown in section 5, finishing in section 6 with the conclusions of this work.

2. Problem under study

The problem that is going to be studied is the compaction of several plies when the sonotrode is still actuating over them, i.e., the sonotrode vibrates but is not moved along the direction of the fibres.

All the plies of the laminate will be considered uncured. The plies are supposed to be formed by two layers of resin and one layer of fibres, as can be seen in Figure 1, where only two plies have been depicted for the sake of clarity.

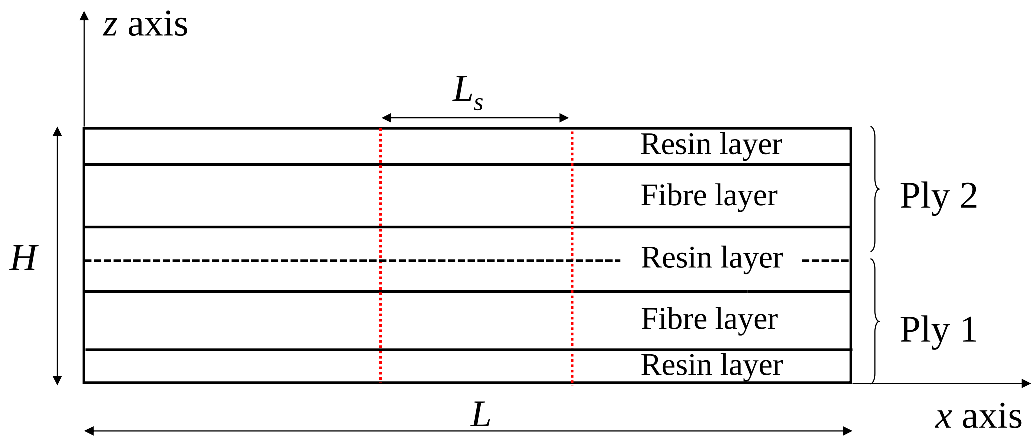

Figure 1. Geometry of the problem

The area of the resin layers under the sonotrode, with a length along the *x* axis of L_s, is where the heat is generated due to the ultrasonic vibration.

The boundary conditions of the problem are:

- Conduction with the sonotrode at the top resin layer at $\frac{1}{2}L - \frac{1}{2}L_s \leq x \leq \frac{1}{2}L + \frac{1}{2}L_s$
- Convection with the air at the top resin layer at $\frac{1}{2}L - \frac{1}{2}L_s > x$; $\quad x > \frac{1}{2}L + \frac{1}{2}L_s$
- Isolation at the other boundaries (note that the temperature far enough from the sonotrode will be equal to room temperature and, under the bottom layer, an isolating material is placed).

3. Coupling the heat generation and distribution

The thermal problem of the heat generation and distribution during the ultrasonic compaction is given by the heat equation as:

$$\rho C_P \frac{\partial T}{\partial t} - \nabla \cdot (\mathbf{K} \nabla T) = \mathbf{Q}^{visc} \tag{1}$$

where $T(x,z,t)$ is the temperature at each point, ρ is the density of the material, C_P is the specific heat capacity of the material, $\mathbf{K}$ is the conductivity tensor of the material and $\mathbf{Q}^{visc}(x,z,t)$ is the heat generation due to internal viscosity of the resin, produced by the ultrasonic vibration.

The transient model will be defined in a plate domain, given by $\Xi = \Omega \times I \times \Gamma$ with $\Omega = [0, L]$, $I = [0, H]$ and $\Gamma = [0, t_{\max}]$, $t_{\max}$ being the maximum time of the process.

The laminate is considered to be composed of P different orthotropic layers, each one characterized by a well defined conductivity tensor $\mathbf{K}_j$ (*j* being the ply), assumed constant through the layer thickness, diagonal and defined in its principal directions by k_x and k_z. In this way, a characteristic function representing the position of each layer can be defined:

$$\chi_j(z) = \begin{cases} 1 & z_j \leq z \leq z_{j+1} \\ 0 & otherwise \end{cases} \qquad j = 1, \ldots, P \tag{2}$$

where $z_j = (j-1) \times h$.

The laminate conductivity can be written in the following separated form using (2):

$$\mathbf{K}(x,z) = \sum_{j=1}^{P} \mathbf{K}_j(x) \chi_j(z) \tag{3}$$

In the case of the other properties of the material, ρ and C_P, a similar separated form is applied.

The same idea can be applied to the heat generation, but using a function $\gamma_j(z)$ that becomes null at the fibre layers. The separated representation of the heat generated can be expressed as:

$$\mathbf{Q}^{visc}(x,z,t) = \sum_{j=1}^{P} \phi_j(x) \gamma_j(z) Q_j(t) \tag{4}$$

Note that $\phi_j(x)$ is a function that takes the value of 1 when *x* is located under the sonotrode and 0 when *x* is not located under the sonotrode.

The problem of the heat generation has been solved in [3]. The equations that govern this generation are presented next. Note that the *x* and *z* coordinates that appear in these equations are different for each resin layer and only concerns the volumes contained in each resin layer.

$$
\begin{aligned}
Q_P(t) &= \int_{-\frac{1}{2}h_P}^{\frac{1}{2}h_P} \int_{-\frac{1}{2}L_S}^{\frac{1}{2}L_S} Q_P^h(x,z,t)\,dxdz + \int_{-\frac{1}{2}h_P}^{\frac{1}{2}h_P} \int_{-\frac{1}{2}L_S}^{\frac{1}{2}L_S} Q_P^v(x,z,t)\,dxdz \\
Q_j(t) &= \int_{-\frac{1}{2}h_j}^{\frac{1}{2}h_j} \int_{-\frac{1}{2}L_S}^{\frac{1}{2}L_S} Q_j^v(x,z,t)\,dxdz \qquad\qquad j = 1,\dots,P-1
\end{aligned} \tag{5}
$$

where:

$$
Q_P^h(x,z,t) = \eta_P(t)\left(\frac{w_{sh}(t)}{h_P}\right)^2 \tag{6}
$$

$$
Q_j^v(x,z,t) = \frac{144\eta_j(t)}{\left(h_j\right)^6}\left[v_j\left(-\tfrac{1}{2}h_j,t\right) - v_j\left(\tfrac{1}{2}h_j,t\right)\right]^2 z^2 x^2 \tag{7}
$$

$Q_P^h(x,z,t)$ being the heat generated due to the horizontal movement of the sonotrode, only generated inside the top layer P, $Q_j^v(x,z,t)$ the heat generated due to the vertical movement of the sonotrode, $\eta_j(t)$ the viscosity of the j^{th}-layer, v_j the vertical velocity of the resin layer at the extremes of the j^{th} -layer, h_j the thickness of the j^{th} -layer and $w_{sh}(t)$ the horizontal component of the velocity of the sonotrode.

Note that the heat generation presents a strong coupling between the layers, through their vertical velocities.

In this case, equation (1) will be solved using a fixed point algorithm. In a first step, assuming that the temperature field is known, the heat generation will be obtained using equations (5), (6) and (7). Once solved, in a second step, the temperature field will be obtained solving equation (1), using the PGD equations that will be presented in the next section. This temperature field leads to a new heat generated, that will be compared with the one obtained in the previous step. The algorithm is continued until reaching the convergence of the heat generated.

4. Governing equations for the PGD solution

The equations that solve the heat distribution (1) along spatial and time (the model is a transient one) coordinates using the Proper Generalized Decomposition are presented next.

The weighted residual form of Eq. (1) can be written as:

$$
\int_{\Xi} T^*\left(\rho C_P \frac{\partial T}{\partial t} - \nabla\cdot\left(\mathbf{K}\nabla T\right) - \mathbf{Q}^{visc}\right) d\Xi = 0 \tag{8}
$$

with the test function T^* defined in an appropriate functional space.

Using the considerations made for the conductivity tensor, equation (8) can be written as:

$$\int_{\Xi} T^* \left(\rho C_P \frac{\partial T}{\partial t} - k_x \frac{\partial^2 T}{\partial x^2} - k_z \frac{\partial^2 T}{\partial z^2} - \mathbf{Q}^{visc} \right) d\Xi = 0 \tag{9}$$

In order to take into account the boundary conditions in the formulation, the equation will be solved integrating by parts the terms that involve second order derivatives.

The boundary conditions were defined in section 2 of this work and can be expressed as:

$$\begin{aligned} &\left.\frac{\partial T}{\partial x}\right|_{x,z\in\Phi_1} = 0 \\ &\left.\frac{\partial T}{\partial z}\right|_{x,z\in\Phi_2} = 0 \\ &\left.\frac{\partial T}{\partial x}\right|_{x,z\in\Phi_3} = 0 \\ &-k_z \left.\frac{\partial T}{\partial z}\right|_{x,z\in\Phi_4} = \begin{cases} h\left(T(x,z=H,t) - T_{amb}\right) & x \in \Phi_4^s - \Phi_4^s \\ h_s\left(T(x,z=H,t) - T_s\right) & x \in \Phi_4 \end{cases} \end{aligned} \tag{10}$$

$\Phi = \partial(\Omega \times I)$ being the whole boundary, defined by $\Phi = \Phi_1 \cup \Phi_2 \cup \Phi_3 \cup \Phi_4$, $\Phi_1 = (x = 0, z \in I)$, $\Phi_2 = (x \in \Omega, z = 0)$, $\Phi_3 = (x = L, z \in I)$, $\Phi_4 = (x \in \Omega, z = H)$. In equations (10), Φ_4^s is the area of Φ_4 located under the sonotrode, h is the convection coefficient and h_s is a coefficient that determines the heat transfer with the sonotrode (this coefficient depends on the conductivity and the geometry of the sonotrode and has been calibrated experimentally).

Equation (9), integrated by parts and including the boundary conditions, can be written as:

$$\begin{aligned} &\int_{\Xi} T^* \rho C_P \frac{\partial T}{\partial t} d\Xi + \int_{\Phi_4 - \Phi_4^s} T^* h\left(T(x,z=H,t) - T_{amb}\right) dxdt + \\ &+ \int_{\Phi_4^s} T^* h_s\left(T(x,z=H,t) - T_s\right) dxdt + \int_{\Xi} k_x \frac{\partial T^*}{\partial x}\frac{\partial T}{\partial x} d\Xi + \int_{\Xi} k_z \frac{\partial T^*}{\partial z}\frac{\partial T}{\partial z} d\Xi - \\ &- \int_{\Xi} T^* \mathbf{Q}_j^{visc} d\Xi = 0 \end{aligned} \tag{11}$$

The solution of equation (11), $T(x,z,t)$, is searched under the separated form:

$$T(x,z,t) \approx \sum_{i=1}^{i=N} X_i(x) \cdot Z_i(z) \cdot \Theta_i(t) \tag{12}$$

In what follows, we are illustrating the construction of one such decomposition, as done in [8]. For this purpose we assume that at iteration $n < N$ the solution is already known:

$$T^n(x,z,t) = \sum_{i=1}^{i=n} X_i(x) \cdot Z_i(z) \cdot \Theta_i(t) \tag{13}$$

and that at the present iteration we look for the solution enrichment:

$$T^{n+1}(x,z,t) = T^n(x,z,t) + R(x) \cdot W(z) \cdot S(t) \tag{14}$$

The test function involved in equation (10) is searched under the form:

$$T^*(x,z,t) = R^*(x) \cdot W(z) \cdot S(t) + R(x) \cdot W^*(z) \cdot S(t) + R(x) \cdot W(z) \cdot S^*(t) \tag{15}$$

The functions $R(x)$, $W(z)$ and $S(t)$ will be obtained with an alternating direction fixed point algorithm. Thus, assuming two of the functions known, the third is calculated. Once done, this function is used in the calculation of the other, iterating until reaching convergence. The converged solutions define the next term in the finite sums decomposition: $R(x) \to X_{n+1}(x)$, $W(z) \to Z_{i+1}(z)$ and $S(t) \to \Theta_{n+1}(t)$.

5. Results

The problem that will be solved is the compaction of 8 unidirectional pre-preg plies, i.e., 9 resin layers and 8 fibre layers. All the layers have been laid-up and are supposed to be uncured, so the heat generation will affect to all of them.

The boundary conditions are those described in Eq. (10). The mesh used consists on 100 nodes along the x axis (the length of the laminate being $L = 60$ mm and the length of the sonotrode $L_s = 20$ mm), 321 nodes along the z axis (the thickness being $H = 1.04$ mm) and 456001 nodes along the time axis (the time of the process being $t_{\max} = 10$ seconds).

The convergence of the solution was reached after adding 25 sums of products of functions $X_i(x)Z_i(z)\Theta_i(t)$. The temperature distribution inside the laminate for $t = 1$ second is shown in Figure 2.

It can be appreciated that there is almost no variation throughout the z direction. The maximum temperature is reached at the zone under the sonotrode, decreasing at its sides until reaching the temperature of the borders of the laminate.

In order to check the accuracy of the solution, a comparison with an experimental measurement has been done. The experimental and numerical evolution of the temperature in time at the bottom of the laminate is presented in Figure 3.

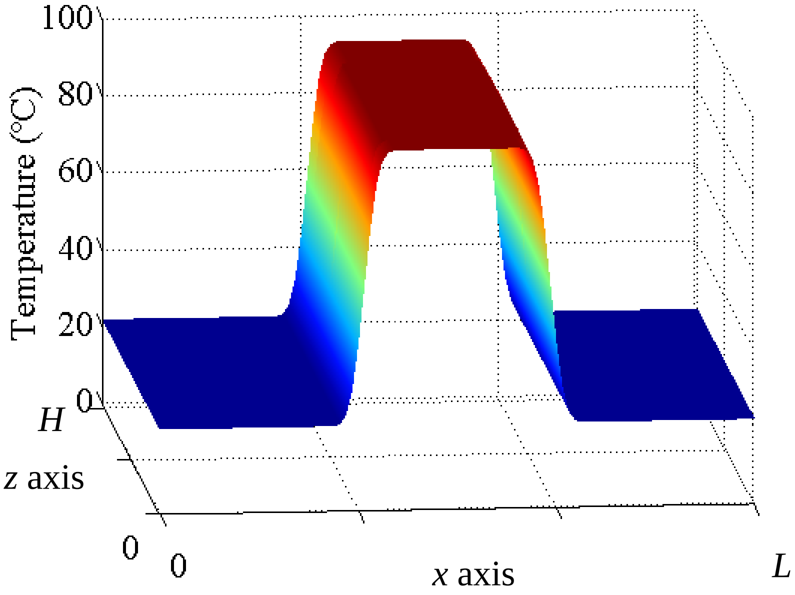

Figure 2. Temperature distribution inside the laminate during compaction process

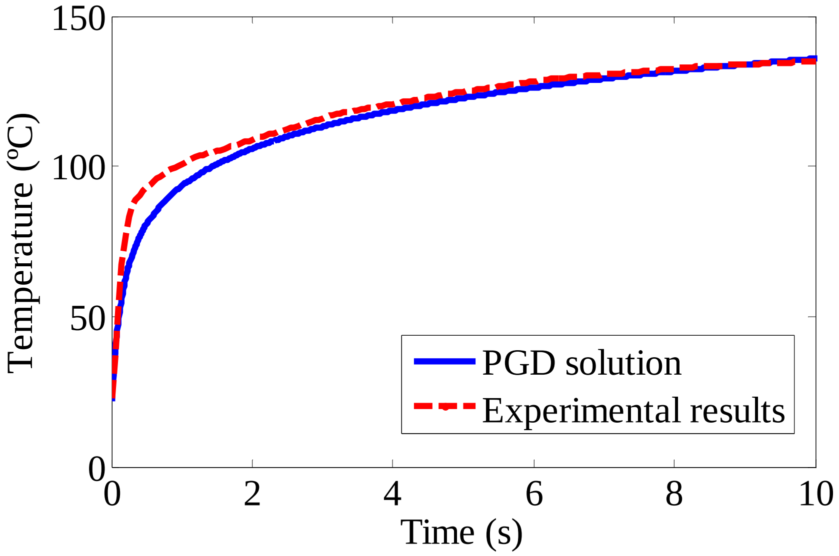

Figure 3. Comparison of experimental and numerical temperature/time curve at the bottom of the laminate

As can be seen, the agreement of the numerical model predicts correctly the experimental behavior.

6. Conclusions

The evolution of the temperature inside a composite laminate during the ultrasonic compaction has been studied. To this end, the problem of the heat generated and distributed has been solved, obtaining the solution of the transient heat equation.

Once the problem under study has been presented, the resolution of the heat equation has been posed. It has been carried out using a fixed point algorithm, on one side solving the heat generated with the equations of [3] and, on the other side, solving the heat distribution with the PGD equations presented in this work.

The governing equations that solve the heat distribution using the PGD have been shown, proposing, again, a fixed point algorithm to obtain the approximation functions.

The solution of the temperature field inside the laminate for a certain number of uncured layers and for a certain value of the time of the process has been depicted.

Finally, the model has been compared with experimental measurements, showing that it can predict the temperature of the laminate along the compaction process with a high accuracy.

The next step of this work could be the modeling of the compaction process when the sonotrode is moved along the laminate.

Acknowledgements

The authors want to thank the EADS Chair of Seville and the EADS and ESI Chairs of Nantes their collaboration in this work.

References

[1] K. Sanjay. Composites Manufacturing. Materials, Product, and Process Engineering. *CRC Press. Mazumda*, 2002.
[2] H. Degrand, F. Cazaux, X. Coqueret, B. Defoort, F. Boursereau and G. Larnac. Thermal effects on the network structure of diglycidylether of bisphenol-A polymerized by electron-beam in the presence of an iodonium salt. *Radiation Physics and Chemistry, 68, Issue 5, 885-891*, 2003.
[3] J. Justo. Curing out of autoclave: development and modelling of an ultrasonic debulking technique. *EADS Chair of Aeronautical Studies*, 2011.
[4] J. Justo, E. Graciani, F. París, R. Ávila. Modeling of ultrasonic tape lamination. *14th European Conference on Composite Materials, Budapest, Hungary*, 2010.
[5] J. Justo, E. Graciani, F. París, F. Chinesta. Study of the heating of pre-preg layers subjected to ultrasonic vibrations. *IX Congreso Nacional de Materiales Compuestos, Spain*, 2011.
[6] F. Chinesta, A. Ammar, A. Leygue and R. Keunings. An overview of the proper generalized decomposition with applications in computational rheology. *Journal of Non-Newtonian Fluid Mechanics, 166, 578-592*, 2011.
[7] A. Ammar, B. Mokdad, F. Chinesta and R. Keunings. A new family of solvers for some classes of multidimensional partial differential equations encountered in kinetic theory modeling of complex fluids. Part II: transient simulation using space-time separated representations. *J. Non-Newtonian Fluid Mech., 144: 98-121*, 2007.
[8] F. Chinesta, A. Leygue, F. Bordeu, J.V. Aguado, E. Cueto, D. Gonzalez, I. Alfaro, A. Ammar, A. Huerta. PGD-Based Computational Vademecum for Efficient Design, Optimization and Control. *Archives of Computational Methods in Engineering, 20, 31–59*, 2013.